A Dynamic Hormone-Cycling in Vitro Model for Phase-Specific Pharmacological Evaluation in Adenomyosis

Lingyu Chen *

Stony Brook, New York, US

* Corresponding Author Email: Tiffs-here@outlook.com

Abstract. Adenomyosis is an estrogen-dependent uterine disorder characterized by inflammation, abnormal estrogen receptor signaling, and aberrant smooth-muscle activation and proliferation, all of which fluctuate across different phases of the menstrual cycle. However, conventional in vitro models lack the ability to simulate dynamic hormonal cycling, limiting the study of phase-specific mechanisms and therapeutic responses. This study established a high estradiol-primed human endometrial stromal cell and human uterine smooth muscle cell co-cultured adenomyosis-like model (H-CoC) and applied controlled estradiol/progesterone ratios to simulate proliferative, luteal, and menstrual phases. Tanshinone IIA and Paeonol were applied as a combined herbal intervention. Markers such as COX-2, PGE2, and estrogen receptor (ER-α/ER-β) expression were measured. The model successfully reproduced key features of adenomyosis, including elevated COX-2 and PGE2 levels and phase-dependent alterations in ER-α and ER-β expressions. Herbal treatment exhibited distinct phase-specific regulatory effects. The strongest activity was observed in the proliferative phase and the menstrual phase. A shift toward ER-β predominance was observed during the proliferative phase, whereas both ER-α and ER-β were significantly suppressed during the menstrual phase, consistent with reduced COX-2, PGE2, and Ki-67 levels, reflecting coordinated anti-inflammatory and anti-proliferative effects. This study establishes a physiologically relevant platform that captures adenomyosis- and menstrual cycle-related pathogenetic changes, and highlights the phase-dependent nature of herbal responsiveness under different hormonal contexts. This system provides a foundation for future in vivo validation and patient-derived organoid studies, supporting cycle-informed evaluation of non-hormonal therapeutic candidates.

Keywords: Adenomyosis, Estrogen Receptor, co-culture model, Menstrual Cycle Regulation, Herbal Medicine.

1. Introduction

Adenomyosis is a common, chronic, invasive uterine disease in which endometrial glands are present within the myometrium [1]. Although the cause is not fully understood, several critical pathological mechanisms, including estrogen dependence, progesterone resistance, chronic inflammation, and smooth muscle activation with hyperplasia-like remodeling and hypertrophy. Clinically, adenomyosis is associated with dysmenorrhea, heavy menstrual bleeding, infertility, and recurrent pregnancy loss [2]. Current medical treatments, mainly hormonal agents and surgery, are limited by androgenic or hypoestrogenic side effects, lack of standardized therapeutic guidelines, and the risk of compromising fertility [3]. Importantly, few therapeutic strategies account for the menstrual phase–dependent fluctuations that characterize the disease.

Hormonal dysregulation plays a central role in adenomyosis pathogenesis. Compared with healthy myometrium, adenomyotic tissue shows elevated estrogen receptor (ER) expression, particularly ER-α, which has been linked to enhanced inflammatory signaling and altered estrogen responsiveness. Increased local aromatase activity further amplifies estradiol synthesis and estrogen signaling within lesions [4,5]. Estrogens also upregulate Bcl-2, an anti-apoptotic protein that supports cellular proliferation across the menstrual cycle [6]. In parallel, progesterone resistance is widely observed in adenomyosis and contributes to the failure of progesterone to counterbalance estrogen-driven proliferation and inflammation. Epigenetic downregulation of progesterone receptor PR-B has been reported in adenomyotic stromal cells, and ER-β–associated regulatory mechanisms have been implicated in this process in certain experimental contexts [7]. Together, enhanced estrogen signaling

and impaired progesterone responsiveness promote myometrial invasion, inflammation, and abnormal tissue remodeling, highlighting estrogen receptor modulation as an important therapeutic target.

Under physiological conditions, ER-α rises during the proliferative phase in response to increasing estrogen levels and decreases during the luteal phase due to progesterone-mediated downregulation [5]. Although ER-β expression is generally lower than ER-α throughout the cycle [8], ER-β expression increases and peaks in the luteal phase [9]. In adenomyotic pathogenesis, ER-α expression predominates [10], whereas ER-β is described as upregulated in certain lesion contexts [11], though findings remain heterogeneous across studies and tissue subregions. ER-β dysregulation has been associated with altered estrogen signaling; it may contribute to lesion biology in a context-dependent manner rather than acting solely as a protective isoform in disease states [12].

To better observe cell-cell interactions in adenomyosis, many three-dimensional co-culture models have been developed, including epithelial organoids, synthetic biomaterial matrices for epithelial–stromal coculture, engineered smooth muscle 3D constructs, engineered microvascular tissue, and a microfluidic platform [13]. While these advanced systems provide improved structural complexity, many remain technically limited in supporting long-term, controlled hormonal cycling required for systematic phase-dependent pharmacological evaluation. In this study, a Transwell-based co-culture system was therefore employed to enable stable endometrial stromal–myometrial communication under precisely controlled estradiol/progesterone ratios, providing a practical platform for examining phase-specific drug effects.

Tanshinone IIA (Tan IIA) and Paeonol were selected as natural herbal compounds due to their well-documented anti-inflammatory and estrogen-modulatory activities. Tan IIA has been reported to influence ER-related signaling, downregulate COX-2 expression, and exhibit selective estrogen receptor modulator–like properties [14-16]. It also reduces cell viability, induces apoptosis, and suppresses migration and invasion in adenomyosis models by downregulating 14-3-3ζ [17]. Paeonol also significantly downregulated COX-2 and PGE2 expression [18], thereby suppressing inflammatory responses by inhibiting CXCR3-mediated signaling [19]. These properties make the combination well-suited for evaluating phase-dependent pharmacological responses within the model's dynamic hormonal environment.

Therefore, this study aimed to establish a model integrating high-estrogen induction and interactions among human endometrial stromal cells and human uterine smooth muscle cells, capable of simulating hormonal transitions during the menstrual cycle, and to use this system to evaluate the phase-specific effects of Tanshinone IIA and Paeonol on estrogen signaling, inflammation, and proliferation.

2. Methodology

2.1. Overview

This study aimed to establish an *in vitro* adenomyosis-like model through a dynamic co-culture system that mimics hormonal fluctuations across the menstrual cycle, and to evaluate the phase-dependent therapeutic effects of Tanshinone IIA and Paeonol. A Transwell-based co-culture of human endometrial stromal cells (hESCs) and human uterine smooth muscle cells (hUtSMCs) was used to simulate endometrial-myometrial interactions that contribute to adenomyosis pathogenesis. The experimental workflow consisted of: 1) Establishing baseline culture models and inducing an adenomyosis-like pathological state under high-estrogen stimulation; 2) Applying simulated menstrual-cycle hormonal conditions; 3) Administering herbal treatment at each hormonal phase. A schematic overview is shown in Figure 1.

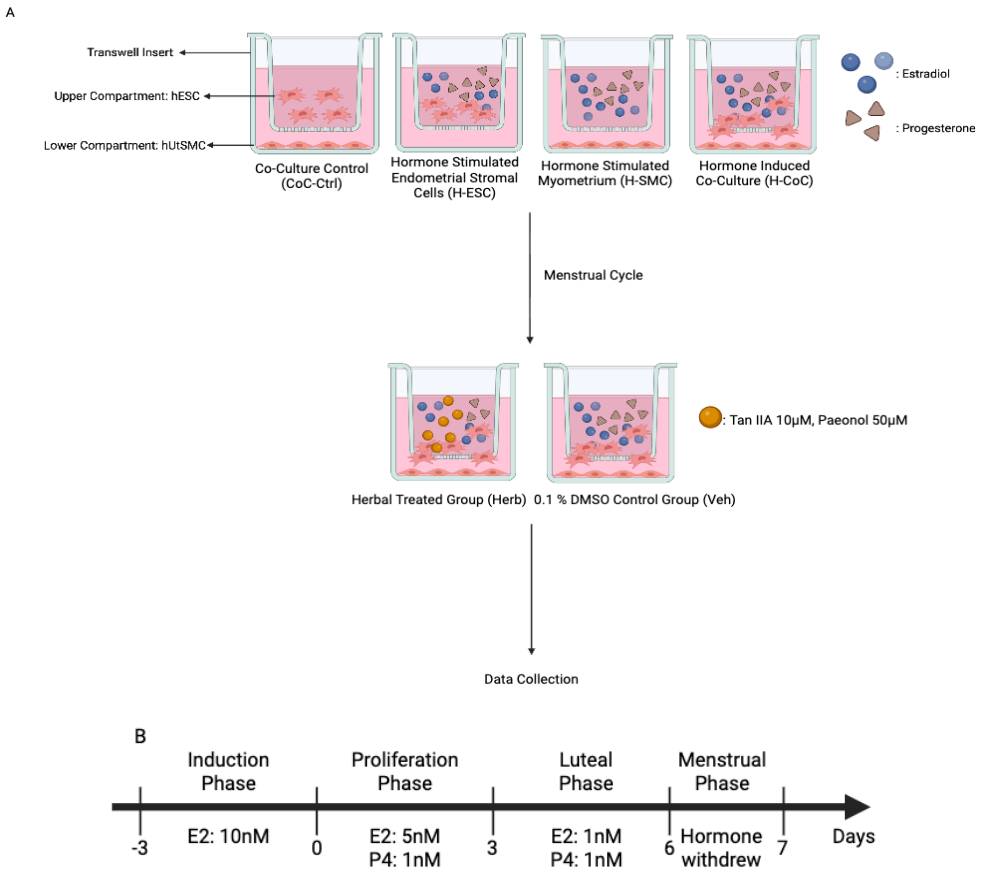

Figure 1. Experimental Design of an *in vitro* adenomyosis-like model and herbal treatment.
(A) Schematic overview of experimental workflow
(B) Timeline of experimental protocol

First, a Transwell-based endometrial–myometrial co-culture system was established with hESCs in the upper compartment and hUtSMCs in the lower compartment. Within this system, a hormone-induced co-culture (H-CoC) was generated by treating the co-culture with estradiol (E2, 10 nM) and progesterone (P4, 1 nM in 0.1% DMSO). Three control conditions were included: a hormone-free co-culture (CoC-Ctrl), a hormone-stimulated endometrial stromal cells monoculture (H-ESC; hESCs treated with the same E2/P4 regimen), and a hormone-stimulated myometrium monoculture (H-SMC). The H-CoC condition exhibited more pronounced adenomyosis-like features than both controls and was therefore selected for the second phase of the study. In this phase, *in vitro* menstrual-cycle stages were simulated by applying phase-specific E2/P4 ratios corresponding to the proliferative, luteal, and menstrual phases. Tanshinone IIA and Paeonol were administered at each phase to evaluate potential phase-dependent therapeutic effects.

2.2. Methods

2.2.1 Cell Co-culture System and Drug Administration

Human endometrial stromal cells (hESC, SNP-H370) and human uterine smooth muscle cells (hUtSMC, SNP-H372) were obtained from Sunncell Biotechnology Co., Ltd. (Wuhan, China). The hESCs and hUtSMCs were co-cultured in Corning® Transwell® 6-well plates (CLS3450, Corning, NY, USA) with 0.4 μm pores at 37 °C and 5% CO_2.

After the cell reached 80% confluency, it was resuspended with trypsin. Parallel pre-coated (with 0.01% Poly-L-Lysine) slides were placed into each well to prepare for immunofluorescence (IF) staining on the cells. 2mL of the hUtSMCs with a density of 3.0×10^5 cells/mL were seeded in the lower compartment of the Transwell system. The cells would attach and grow overnight at 37°C, 5% CO_2. The hESCs were seeded onto the insert chamber at a density of 2.0×10^5 cells per insert, and after 24 hours, the inserts were transferred into corresponding 6-well plates containing the pre-seeded

hUtSMCs to initiate co-culture. The cells would then be co-cultured for 72 hours, during which 10nM estradiol (HY-B0141, MedChemExpress) was administered to the Transwell system to induce a high-estrogen pathological environment. After the 72-hour high-estrogen induction period, the co-culture was exposed to phase-specific E2 and P4 (HY-N0437, MedChemExpress) concentrations to simulate the menstrual cycle. Hormonal dosing (follicular phase: 5nM E2 + 1nM P4; luteal phase: 1nM E2 + 1nM P4; menstrual phase: E2, P4 withdrawn) was adapted from published *in-vitro* models that scale physiological serum ranges to effective cellular concentrations [20].10μM tanshinone IIA (HY-N0135, MedChemExpress) and 50μM paeonol (HY-N0159, MedChemExpress) were given in each phase. Cells were harvested on Day 8 for downstream analyses. All hormone and drug treatments were prepared in 0.1% DMSO, which served as the vehicle control.

2.2.2 Immunofluorescence (IF)

The cells were fixed with 4% formaldehyde, permeabilized, and blocked with PBS containing 10% goat serum, 0.3 M glycine, 1% BSA, and 0.1% Tween. Samples were incubated overnight at 4°C with either rabbit anti-α-SMA or anti-COX-2 /Cyclooxygenase 2 antibody (1:100, ab179800, Abcam) primary antibodies, followed by Goat Anti-Rabbit Alexa Fluor 647–conjugated secondary antibody (1:200 ab150079, Abcam) for 2 h at room temperature. Nuclei were counterstained with DAPI (P0131, Beyotime) and images were acquired using a confocal fluorescent microscope (FV3000, Olympus).

2.2.3 Real-time Polymerase Chain Reaction (Real-time PCR)

The RNA of hESCs was collected with 1mL FastPure Cell/Tissue Total RNA Isolation Kit V2 (TRIzol, RC112-01, Vazyme) according to the manufacturer's instructions. cDNA was synthesized from 50 ng RNA using HiScript III 1st Strand cDNA Synthesis Kit (+gDNA wiper) (R312-01, Vazyme). Reaction mixtures were incubated at 50°C for 45 minutes and 85°C for 2 minutes. ChamQ SYBR Color qPCR Master Mix (Without ROX) (Q421-02, Vazyme) was used to perform real-time PCR based on SYBR Green I fluorescence. The primer sequence was as follows: KI67-F: ACG CCT GGT TAC TAT CAA AAG G; KI67-R: CAG ACC CAT TTA CTT GTG TTG GA. GAPDH was used as the reference gene, and samples were measured using the T100 Thermal Cycler (Bio-Rad). Relative mRNA levels were calculated using the $2^{-\Delta\Delta CT}$ method and expressed as a percentage of the vehicle control.

2.2.4 Western Blot (WB)

Proteins were extracted from hUtSMCs using WB/IP lysis buffer (20118ES60, Yeasen). Equal amounts of protein were separated on a 10% SDS-PAGE gel and transferred to PVDF membranes. After blocking, membranes were incubated at 4°C overnight with primary antibodies: rabbit anti-estrogen receptor alpha antibody (1:20000, ab108398, Abcam), anti-estrogen receptor beta 1 antibody (1:20000, ab187291, Abcam), and mouse anti-beta Actin antibody (1:20000, ab6276, Abcam). HRP-labeled Goat Anti-Rabbit IgG (H+L) (1:1000, A0208, Beyotime) and HRP-labeled Goat Anti-Mouse IgG (H+L) (1:1000, A0216, Beyotime) were used as secondary antibodies. Chemiluminescence was visualized through Super ECL Detection Reagent (36208ES60, Yeasen) and developed on a chemiluminescent imaging system (Tanon 4600SF).

2.2.5 ELISA

Prostaglandin E2 Parameter Assay Kit (KGE004B, R&D System) was used with 50μL medium according to the manufacturer's instructions. BioTek Cytation™3 Cell Imaging Multi-Mode Reader was used as a microplate reader.

2.2.6 Flow Cytometry

The hUtSMCs were fixed with 4% paraformaldehyde and permeabilized with 90% methanol, stained with Anti-alpha smooth muscle Actin antibody (1:1000, ab124964, Abcam) and Goat Anti-Rabbit Alexa Fluor® 488-conjugated secondary antibody (1:500, ab150081, Abcam). Cytoflex and Flowjo were used to analyze the results.

2.2.7 Statistical Analysis

Image analysis was performed using ImageJ. Statistical analyses were conducted in GraphPad Prism using Student's t-test or one-way ANOVA, followed by appropriate post hoc multiple comparison tests. Data are presented as the mean ± SEM. $P < 0.05$ was considered statistically significant.

3. Results

3.1. Establishment and validation of an adenomyosis-like model *in vitro*

The adenomyosis-like co-cultured model (H-CoC) exhibited stronger adenomyosis-like features than all control groups under high estradiol (10nM). Immunofluorescence showed markedly elevated COX-2 expression in H-CoC compared with H-ESC (H-ESC: 24.4 ± 3.04; H-CoC: 276.4 ± 41.4; p = 0.0255) (Fig. 2A- B). Consistently, secreted PGE2 levels were significantly increased in H-CoC co-culture medium (CoC-Ctrl: 843 ± 41; H-CoC: 4107 ± 203.9; p < 0.0001) (Fig. 2C), confirming an enhanced inflammatory response in the co-culture system. Western blot analysis showed that ER-α expression was significantly upregulated in both H-CoC and H-SMC compared with their respective controls (p = 0.0002). In contrast, ER-β expression was markedly higher in H-CoC than in both control groups (p < 0.0001), indicating that stromal–smooth muscle interaction under high estrogen was associated with preferential enhancement of ER-β expression. This shift resulted in a relative increase in ER-β predominance despite overall elevated ER-α levels, suggesting a hormone-responsive receptor rebalancing characteristic of adenomyosis-like tissues (Fig. 2D). Flow cytometry further demonstrated a substantial increase in α-SMA$^+$ smooth-muscle cells in H-CoC relative to myometrial controls (p < 0.0001) (Fig. 2E). indicating stronger smooth-muscle activation and fibrotic-like remodeling. In addition, Ki-67 expression was significantly higher in H-CoC compared with H-ESC controls (fold change = 2.12, p = 0.029) (Fig. 2F), reflecting enhanced proliferative activity.

Altogether, high-estrogen co-culture induces stronger inflammation, proliferation, estrogen-receptor imbalance, and smooth-muscle activation than either monoculture or hormone-free co-culture, supporting H-CoC as a robust and physiologically relevant *in-vitro* adenomyosis-like model.

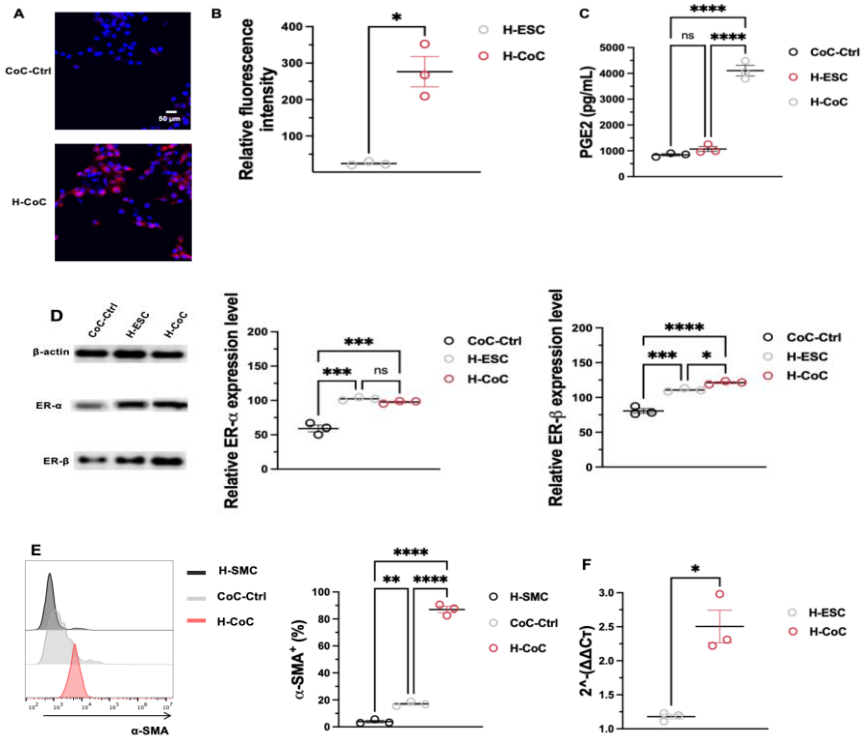

Figure 2. Validation of the *in vitro* high-estrogen co-culture (H-CoC) adenomyosis-like model.

(A) Representative immunofluorescence staining of DAPI (blue) and COX-2 (red) in the CoC-Ctrl and H-CoC groups. Scale bar: 50 μm, magnification: 20x.

(B) Quantification of relative COX-2 fluorescence intensity showing higher expression in the H-CoC model ($p = 0.0255$).

(C) PGE2 concentrations measured by ELISA in CoC-Ctrl, H-ESC, and H-CoC groups.

(D) Representative WB images and quantification of relative ER-α and ER-β expression level normalized to β-actin.

E) Flow cytometry histograms and quantification of α-SMA$^+$ hUtSMC in the myometrial control, CoC-Ctrl, and H-CoC groups.

F) qPCR quantification of Ki-67 expression. Data are presented as mean ± SEM, n = 3. *: $p < 0.05$; **: $p < 0.01$; ***: $p < 0.001$; ****: $p < 0.0001$.

3.2. Herbal treatment modulates ER signaling in a phase-dependent manner

In the vehicle (Veh) group, ER-α and ER-β expression varied following clear phase-dependent patterns (Fig. 3B). Both ER-α and ER-β gradually increased from induction to the menstrual phase, with the highest levels observed during menstruation. ER-β rose slightly more steeply than ER-α, resulting in modest fluctuations in the ER-α/ER-β ratio (0.70–1.04) across phases (Fig. 3A-B). In the proliferative phase, the vehicle group demonstrated a shift toward ER-α predominance, reflected by an ER-α/ER-β ratio of 1.04, suggesting increased estrogen responsiveness during proliferative activation. In subsequent luteal and menstrual phases, ER-β overtook ER-α, indicating a shift toward a progesterone-responsive and tissue-repair-associated signaling profile.

Herbal treatment altered these hormone-dependent dynamics in a phase-specific manner. In the proliferative phase, treatment reversed the ER imbalance observed in the vehicle group, shifting from an ER-α-dominant profile (Veh ratio: 1.04) to an ER-β-dominant state (Herb ratio: 0.61). This rebalanced ER pattern is consistent with the reported biological role of ER-β in moderating estrogen-driven proliferation. In the menstrual phase, herbal treatment markedly reduced the expression of both ER-α and ER-β (47.19 ± 2.68 and 41.33 ± 4.61, respectively), indicating strong suppression of estrogen-responsive signaling. While the ER-α/ER-β ratio increased (Veh: 0.76; Herb: 1.14), this shift occurred under conditions of globally reduced receptor expression. Thus, the ratio change reflects a relative effect rather than a true increase in ER-α-driven signaling.

3.3. Herbal treatment suppressed the inflammation and proliferation induced by high estrogen levels

Inflammatory marker changes paralleled the phase-dependent dynamics of ER signaling. COX-2 fluorescence intensity in the Veh group progressively increased and reached its peak during the menstrual phase (Fig. 3C–D), indicating the strongest inflammatory response at this stage. Herbal treatment significantly reduced COX-2 levels, especially during the menstrual phase, effectively preventing the menstruation-related inflammatory surge. A modest increase in COX-2 was observed in the proliferative phase after treatment, consistent with the heightened estrogen responsiveness characteristic of this stage. PGE2 secretion followed a similar pattern: the H-CoC model showed phase-dependent elevation, with a pronounced peak during the menstrual phase. Herbal treatment markedly reduced PGE2 level across all phases (Fig. 3E), demonstrating a consistent anti-inflammatory effect. Cell proliferation showed comparable phase-dependent trends. Ki-67 expression was substantially increased in the vehicle group but significantly suppressed following herbal treatment, particularly in the proliferative and menstrual phases (Fig. 3F), indicating attenuation of estrogen-driven proliferative activity.

Together, these findings demonstrate that the herbal combination exerts phase-specific modulation of estrogen-receptor balance and inflammatory and proliferative activity, with the most notable therapeutic responses occurring during the proliferative and menstrual phases.

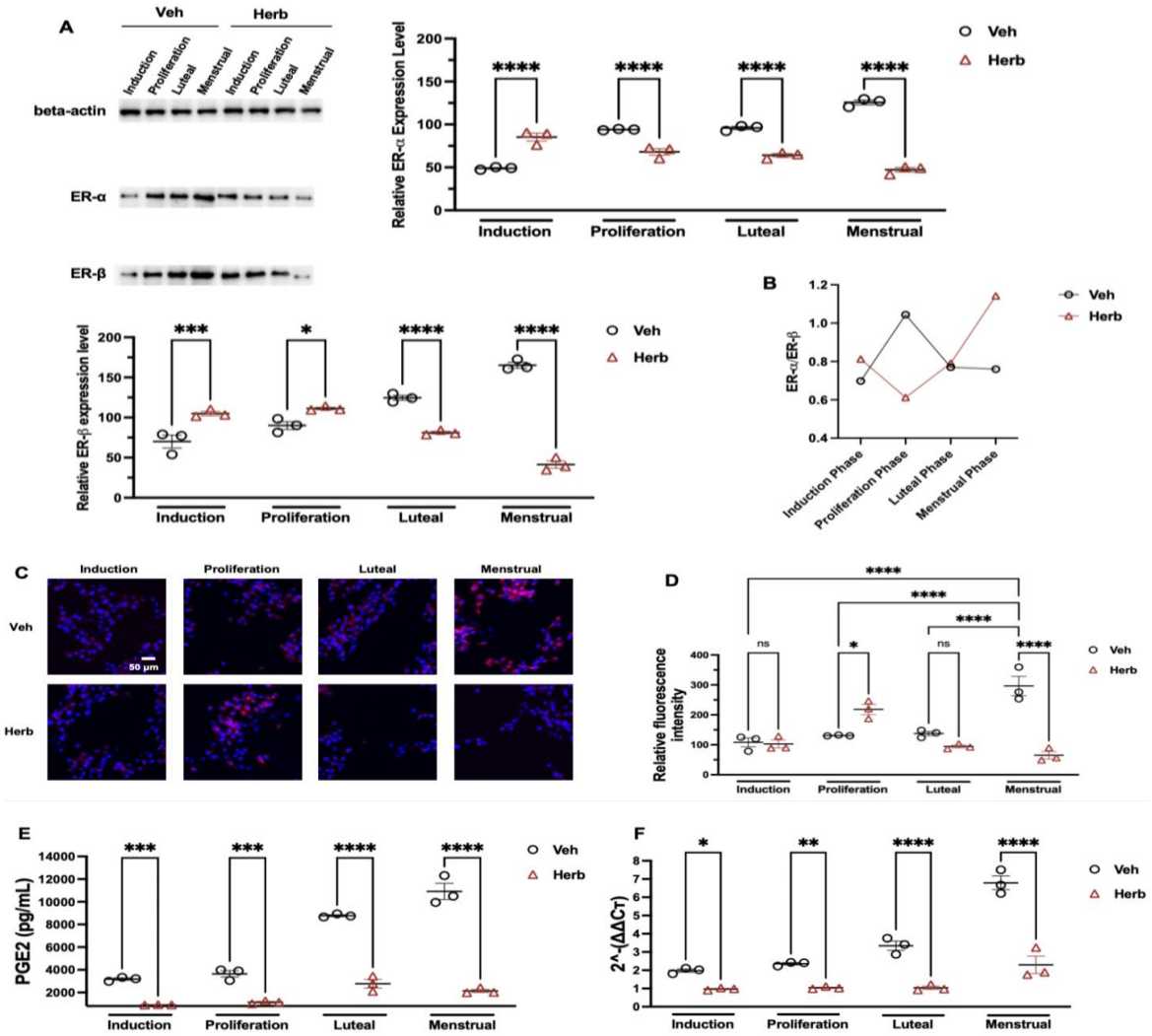

Figure 3. Phase-dependent effects of herbal treatment on ER signaling, inflammation, and proliferation.

(A) Representative WB analysis images and quantification of ER-α and ER-β expression across hormonal phases in the co-culture model.

(B) ER-α/ER-β ratio calculated for vehicle (Veh) and herbal treatment (Herb) groups.

(C) Representative immunofluorescence images of DAPI (blue) and COX-2 (red) under different hormonal phases.

(D) Quantification of relative COX-2 fluorescence intensity.

(E) PGE2 concentration measured by ELISA.

(F) Ki-67 mRNA expression quantified by qPCR. Data are presented as mean ± SEM. *: $p < 0.05$; **: $p < 0.01$; ***: $p < 0.001$; ****: $p < 0.0001$.

4. Conclusion

The *in vitro* adenomyosis-like co-culture model established in this study successfully simulated phase-specific hormonal conditions across the menstrual cycle by integrating human endometrial stromal cells and uterine smooth muscle cells under controlled estradiol/progesterone conditions. This dynamic system enables precise evaluation of phase-dependent biological responses and provides a physiologically relevant platform for assessing treatment sensitivity across menstrual phases.

Herbal treatment produced distinct, phase-specific regulatory effects on estrogen receptor signaling. During the proliferative phase, the herbal treatment shifted toward ER-β predominance, a pattern associated with reduced estrogen-driven proliferation. In contrast, during the menstrual phase, both

receptors were markedly suppressed, with a greater reduction of ER-α, corresponding to pronounced decreases in COX-2, PGE2, and Ki-67. These findings demonstrate that herbal intervention modulates ER balance, inflammatory activation, and proliferative behavior in a phase-dependent manner, with the strongest therapeutic effects observed during the proliferative and menstrual phases.

Beyond demonstrating biological relevance, the dynamic co-culture system highlights the importance and feasibility of cycle-informed therapeutic strategies. Since pharmacological responses vary substantially across hormonal contexts, this model provides a platform for exploring phase-dependent treatment responsiveness and for screening agents with phase-dependent therapeutic responsiveness. Future studies should extend these findings using *in vivo* models and human-derived organoid systems to validate the phase-specific effects observed here and to refine the timing of herbal or non-hormonal interventions.

References

[1] Moawad, G., Fruscalzo, A., Youssef, Y., Kheil, M., Tawil, T., Nehme, J., Pirtea, P., Guani, B., Afaneh, H., Ayoubi, J. M., & Feki, A. (2023). Adenomyosis: An updated review on diagnosis and classification. Journal of Clinical Medicine, *12*(14), 4828. https://doi.org/10.3390/jcm12144828

[2] Zhai, J., Vannuccini, S., Petraglia, F., & Giudice, L. C. (2020). Adenomyosis: Mechanisms and pathogenesis. Seminars in Reproductive Medicine, *38*(2-03), 129–143. https://doi.org/10.1055/s-0040-1716687

[3] Etrusco, A., Barra, F., Chiantera, V., Ferrero, S., Bogliolo, S., Evangelisti, G., Oral, E., Pastore, M., Izzotti, A., Venezia, R., Ceccaroni, M., & Laganà, A. S. (2023). Current medical therapy for adenomyosis: From bench to bedside. Drugs, *83*(17), 1595–1611. https://doi.org/10.1007/s40265-023-01957-7

[4] Sztachelska, M., Ponikwicka-Tyszko, D., Martínez-Rodrigo, L., Bernaczyk, P., Palak, E., Półchłopek, W., Bielawski, T., & Wołczyński, S. (2022). Functional implications of estrogen and progesterone receptors expression in adenomyosis, potential targets for endocrinological therapy. Journal of Clinical Medicine, *11*(15), 4407. https://doi.org/10.3390/jcm11154407

[5] Garavaglia, E., Audrey, S., Annalisa, I., Stefano, F., Iacopo, T., Laura, C., & Massimo, C. (2015). Adenomyosis and its impact on women fertility. Iranian Journal of Reproductive Medicine, *13*(6), 327–336.

[6] Lessey, B. A., Palomino, W. A., Apparao, K. B., Young, S. L., & Lininger, R. A. (2006). Estrogen receptor-alpha (ER-alpha) and defects in uterine receptivity in women. Reproductive Biology and Endocrinology, *4*(Suppl 1), S9. https://doi.org/10.1186/1477-7827-4-S1-S9

[7] Matsuzaki, S., Fukaya, T., Suzuki, T., Murakami, T., Sasano, H., & Yajima, A. (1999). Oestrogen receptor alpha and beta mRNA expression in human endometrium throughout the menstrual cycle. Molecular Human Reproduction, *5*(6), 559–564. https://doi.org/10.1093/molehr/5.6.559

[8] Lecce, G., Meduri, G., Ancelin, M., Bergeron, C., & Perrot-Applanat, M. (2001). Presence of estrogen receptor beta in the human endometrium through the cycle: Expression in glandular, stromal, and vascular cells. The Journal of Clinical Endocrinology & Metabolism, *86*(3), 1379–1386. https://doi.org/10.1210/jcem.86.3.7322

[9] Trukhacheva, E., Lin, Z., Reierstad, S., Cheng, Y. H., Milad, M., & Bulun, S. E. (2009). Estrogen receptor (ER) beta regulates ERalpha expression in stromal cells derived from ovarian endometriosis. The Journal of Clinical Endocrinology & Metabolism, *94*(2), 615–622. https://doi.org/10.1210/jc.2008-1466

[10] Maclean, A., Tipple, L., Newton, E., & Hapangama, D. K. (2025). Hormone receptor profile of ectopic and eutopic endometrium in adenomyosis: A systematic review. Human Reproduction Open, *2025*(1), hoaf002. https://doi.org/10.1093/hropen/hoaf002

[11] Burns, K. A., & Korach, K. S. (2012). Estrogen receptors and human disease: An update. Archives of Toxicology, *86*(10), 1491–1504. https://doi.org/10.1007/s00204-012-0868-5

[12] Gnecco, J. S., Brown, A. T., Kan, E. L., Baugh, L., Ives, C., Loring, M., & Griffith, L. G. (2020). Physiomimetic models of adenomyosis. Seminars in Reproductive Medicine, *38*(2-03), 179–196. https://doi.org/10.1055/s-0040-1719084

[13] Zhao, P., Soukup, S., Hegevoss, J., Ngueu, S., Kulling, S., & Diel, P. (2015). Anabolic effect of the Traditional Chinese Medicine compound tanshinone IIA on myotube hypertrophy is mediated by estrogen receptor. Planta Medica, *81*(7), 578–585. https://doi.org/10.1055/s-0035-1545883

[14] Ma, X., Zhang, L., Gao, F., Jia, W., & Li, C. (2023). Salvia miltiorrhiza and tanshinone IIA reduce endothelial inflammation and atherosclerotic plaque formation through inhibiting COX-2. Biomedicine & Pharmacotherapy, *167*, 115501. https://doi.org/10.1016/j.biopha.2023.115501

[15] Fan, G. W., Gao, X. M., Wang, H., Zhu, Y., Zhang, J., Hu, L. M., Su, Y. F., Kang, L. Y., & Zhang, B. L. (2009). The anti-inflammatory activities of Tanshinone IIA, an active component of TCM, are mediated by estrogen receptor activation and inhibition of iNOS. The Journal of Steroid Biochemistry and Molecular Biology, *113*(3-5), 275–280. https://doi.org/10.1016/j.jsbmb.2009.01.011

[16] Wan, L., Zou, Y., Wan, L. H., Wang, L. Q., Huang, M. Z., Wu, J., Zhu, Y. B., & Huang, O. P. (2015). Tanshinone IIA inhibits the proliferation, migration and invasion of ectopic endometrial stromal cells of adenomyosis via 14-3-3ζ downregulation. Archives of Gynecology and Obstetrics, *292*(6), 1301–1309. https://doi.org/10.1007/s00404-015-3766-2

[17] Liu, H., & Zhang, C. (2020). Paeonol induces antitumor effects in hepatocellular carcinoma cells through survivin via the cyclooxygenase-2/prostaglandin E2 signaling pathway. Translational Cancer Research, *9*(11), 7183–7195. https://doi.org/10.21037/tcr-20-322A

[18] Wang, W., Li, Q., Zhao, Z., Liu, Y., Wang, Y., Xiong, H., & Mei, Z. (2022). Paeonol ameliorates chronic itch and spinal astrocytic activation via CXCR3 in an experimental dry skin model in mice. Frontiers in Pharmacology, *12*, 805222. https://doi.org/10.3389/fphar.2021.805222

[19] Ochoa, S., Rasquel-Oliveira, F. S., McKinnon, B., Haro, M., Subramaniam, S., Yu, P., Coetzee, S., Anglesio, M. S., Wright, K. N., Meyer, R., Gargett, C. E., Mortlock, S., Montgomery, G. W., Rogers, M. S., & Lawrenson, K. (2024, November 22). M2 macrophages are major mediators of germline risk of endometriosis and explain pleiotropy with comorbid traits [Preprint]. bioRxiv. https://doi.org/10.1101/2024.11.21.624726

[20] d'Otreppe, J., Patino-García, D., Piekos, P., de Codt, M., Manavella, D. D., Courtoy, G. E., & Orellana, R. (2024). Exploring the endocrine mechanisms in adenomyosis: From pathogenesis to therapies. Endocrines, *5*(1), 46–71. https://doi.org/10.3390/endocrines5010004